Journal of Alloys and Compounds, 190 (1992) 99–106
JALCOM 413

Reaction of samarium with hydrogen and nitrogen samarium oxides

Chris N. Christodoulou and Takuo Takeshita
Central Research Institute, Mitsubishi Materials Corporation, 1-297 Kitabukuro-cho, Omiya, Saitama 330 (Japan)

(Received July 7, 1992)

Abstract

The reaction characteristics between Sm metal and H_2 or N_2 gas have been studied by means of isochorothermal analysis and X-ray diffraction. Samarium was found to react with hydrogen forming SmH_{2+x} ($0 \leqslant x \leqslant 0.63$). The reaction is very abrupt, exothermic and takes place at a temperature of between 300 and 525 °C depending on the initial size, surface contamination and surface structural defects of the samarium metal. Sm hydrides are partially decomposed into b.c.c. Sm_2O_3 under ambient conditions. The reaction of Samarium with N_2 initiates at about 600 °C and proceeds very slowly forming SmN. SmN hydrolyzes in the presence of atmospheric moisture to form b.c.c. Sm_2O_3, hex-$Sm(OH)_3$ and NH_3. Sm oxide surface layers containing f.c.c. SmO, b.c.c. Sm_2O_3 and monoclinic Sm_2O_3 were found to form upon heat treatment of Sm metal under vacuum or argon gas flow.

1. Introduction

The "samarium–hydrogen" system has been studied in terms of its phase diagram [1]; crystal structures of Sm hydrides and phase relationships between SmH_2 and SmH_3 [2, 3]; low temperature thermal expansion of Sm hydrides [4]; and proton self-diffusion and hydrogen-ordering effects [5]. The preparation and crystal structure of SmN have been studied by Eick et al. [6]. Samarium is known to form a series of oxides such as f.c.c. SmO (NaCl-type according to Eick et al. [7] or ZnS-type according to Bist et al. [8]), b.c.c. Sm_2O_3 [9] and monoclinic Sm_2O_3 [10].

The discovery of a new magnetic material, Sm_2Fe_{17} nitride [11], triggered a renewed interest in Sm–Fe intermetallic compounds in general. Permanent magnets based on Sm_2Fe_{17} nitride have already been developed by several methods such as mechanical alloying (MA) [12, 13], rapid quenching [14, 15], conventional powder metallurgy [13, 16, 17] and hydrogen treatment (HDDR) [18, 19]. All of these methods involve two major steps:

(a) the formation of the Sm_2Fe_{17} phase (preferably in a microcrystalline form) and

(b) the nitrogenation of Sm_2Fe_{17} in N_2 or ammonia to form interstitial Sm_2Fe_{17} nitride which is responsible for the hard magnetic properties.

So far many studies have been published based on Sm_2Fe_{17} nitrides and are mainly concerned with the nitrogenation kinetics [20, 21] and substitutions [11, 22–27] of Sm or Fe with other rare earth and transition metals, respectively. In step (a) of the previously mentioned preparation methods, usually one has to deal not only with the major Sm_2Fe_{17} phase but also with other phases such as Sm, $SmFe_2$, $SmFe_3$ and α-Fe. Consequently, in the whole process (steps (a) and (b)) one has to consider the reaction products of these "secondary" phases with hydrogen and nitrogen as well as oxygen. The reaction products have an effect on the details of the processes as well as on the magnetic properties of the final product. Experience of working with other magnetic materials such as the $Nd_2Fe_{14}B$-based magnets shows that the presence of the secondary phases plays an important role in the development of the intrinsic coercivity.

Presently, there is little or no specific information about the kinetics and reaction products between the Sm–Fe alloys and hydrogen or nitrogen. The lack of such information led us to make a series of studies of the reactions between Sm, $SmFe_2$, $SmFe_3$ and Sm_2Fe_{17} single phases, and hydrogen or nitrogen gas as a function of temperature. In the present paper, only the reaction between samarium metal and H_2 or N_2, and some information on the formation of Sm oxides will be reported. The reaction of H_2 and N_2 with the other phases ($SmFe_2$, $SmFe_3$ and Sm_2Fe_{17}) will be reported in the near future. Such information on the reactions between the Sm–Fe alloys and H_2 or N_2 has been used to interpret the resulting phases and magnetic properties of Sm_2Fe_{17} nitride-based permanent magnets prepared in our laboratory by several methods; these will also be published in the near future.

0925-8388/92/$5.00

2. Experimental details

The samarium used in the present study was 99.9 wt.% pure. Samarium metal was used both in the form of powder passed through a sieve of 150 μm mesh and small bulk single pieces. The purity of H_2, N_2 and Ar gases was greater than 99.999 vol.%.

The constant volume reactor isochoro-thermal analyzer (ITA) which was used in the present study is similar to the thermopiezic analyzer (TPA) used by other researchers (for instance, Coey et al. [11]) for the study of gas–solid reactions. The volume of ITA was about 2.3 cm^3 and only about 5% of the total volume was heated. The Sm samples, weighting between 2 and 6 mg, were placed in a quartz tube and heated with a precisely controlled programmable furnace capable of reaching a temperature of 1000 °C. The pressure was measured with a pressure sensor capable of detecting pressure differences of about 100 Pa. The temperature was measured with an accuracy of ± 1 °C. The pressure vs. temperature data was collected in a computer and analyzed by taking into consideration the pressure variations due to the thermal effects (heated volume). By utilizing the ideal gas law, the data was transformed and plotted in terms of atoms of gas absorbed by the solid or desorbed from the solid as a function of temperature. The ideal gas law which was applied in the case of hydrogen and nitrogen is considered to be a very good approximation since the pressure–temperature conditions (0–150 kPa and 20–1000 °C) are far above their corresponding critical pressures and temperatures. ITA isochores were obtained for the "Sm (powder) + H_2 or N_2" and "Sm (bulk) + H_2 or N_2" systems in the temperature range of 20 to 950 °C.

Phase analysis was performed by X-ray powder diffraction. X-ray powder diffraction patterns were obtained under ambient conditions by using a Philips automated diffractometer with a CuKα radiation monochromated by a graphite single crystal.

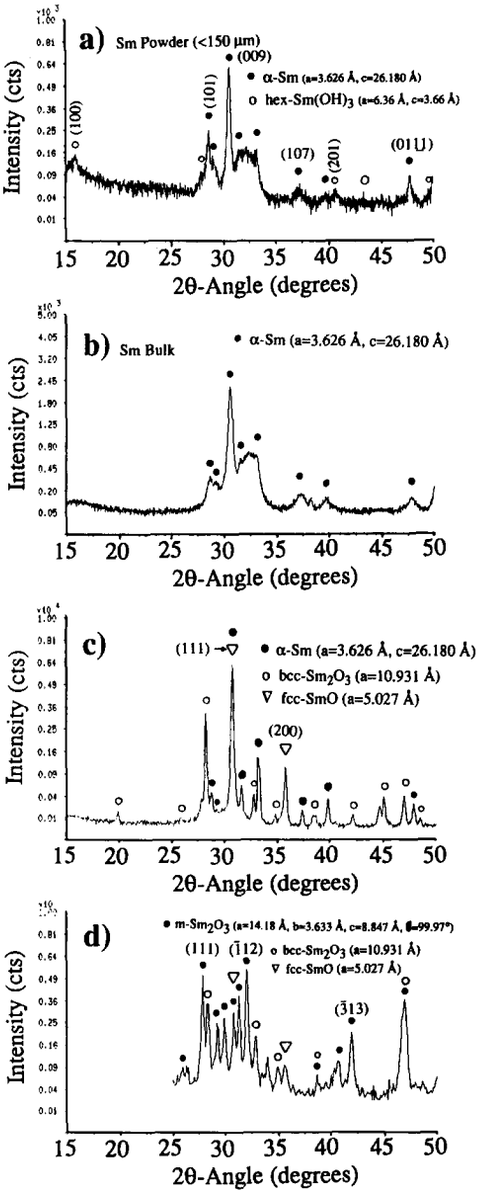

Fig. 1. XRD patterns of (a) Sm powder, (b) bulk Sm, (c) bulk Sm metal heat treated under argon flow at 500 °C for 2 hours, and (d) bulk Sm metal heat treated under vacuum at 800 °C for 1 hour.

3. Results and discussion

3.1. Samarium metal and oxides

3.1.1. The powder and bulk samarium (Sm)

The X-ray diffraction (XRD) patterns for powder and bulk samarium metal used in the present study are shown in Figs. 1(a) and 1(b), respectively. Both exhibit a rhombohedral crystal structure (α-Sm, $a = 3.626$ Å, $c = 26.180$ Å) which is the stable structure of samarium at room temperature [28]. A close inspection of the diffraction pattern of Sm powder (Fig. 1(a)) reveals the existence of a thin surface layer of the hexagonal $Sm(OH)_3$ phase ($a = 6.36$ Å, $c = 3.66$ Å). The broadness of the Bragg peaks between $2\theta = 27.5°$ and $2\theta = 35°$ in both powder and bulk Sm (Fig. 1(a, b)) is an indication of the structural deformation on the surface of Sm metal, apparently caused during the cutting or grinding process. As shown above (Fig. 1(c)), annealing of the Sm metal at 500 °C under argon causes "sharpening" of the Bragg peaks due to the removal of such surface structural defects. Therefore, both powder and bulk Sm as-prepared were structurally deformed on the surface. In addition, the Sm powder surface was covered with a thin layer of $Sm(OH)_3$. No oxides or other surface contamination was observed in the case of bulk Sm which was carefully cut from the bulk of a big Sm

metal chunk. Some chemisorbed oxygen is most likely to be also present in both powder and bulk Sm samples.

3.1.2. Samarium oxides

Figures 1(c, d) show the XRD patterns of a bulk Sm metal (Fig. 1(b)) heat-treated under argon flow at 500 °C for 2 hours (Fig. 1(c)) and in vacuum ($\approx 10^{-6}$ Torr) at 800 °C for one hour (Fig. 1(d)). Both heat treatments (under argon or vacuum) resulted in the formation of f.c.c. SmO ($a = 5.027$ Å) and b.c.c. Sm_2O_3 ($a = 10.931$ Å). In addition, vacuum heat treatment resulted in the formation of monoclinic Sm_2O_3 [3]. Surface polishing of the heat-treated Sm samples removed the Sm oxides and the XRD pattern is the same as that of the initial Sm sample (Fig. 1(b)).

The heat treatment of Sm metal under vacuum or argon gas flow results in the formation of Sm oxide surface layers. The source of oxygen might be both the surface chemisorbed oxygen (which is unavoidable under ambient conditions) and oxygen present as a residue in vacuum or as an impurity in the argon gas. This observation is important because during the preparation (*i.e.* MA and HDDR) of the Sm_2Fe_{17} nitride-based permanent magnets, one has to take into consideration the possible formation of Sm oxides and try to minimize them.

3.2. Reaction of samarium with hydrogen

3.2.1. Hydrogen absorption

The ITA isochore trace of the "Sm(powder) + H_2" system is shown in Fig. 2. On heating, samarium begins to absorb hydrogen abruptly at 330 °C with the hydrogen concentration reaching a value of about 2.17 H atoms per Sm atom. On heating at higher temperatures, hydrogen begins to desorb partially. On cooling, hydrogen is reabsorbed and the final composition of Sm hydride at room temperature (RT) becomes $SmH_{2.14}$. In this sample the final hydrogen concentration is underestimated because during heating at high temperatures (above 850 °C) a portion of Sm is consumed due to reaction with the quartz tube, inside of which the reaction took place. In order to avoid this effect, an ITA isochore was obtained for the "Sm(powder) + H_2" by heating only up to 360 °C and then cooling to RT as shown in Fig. 3. In this experiment, an $SmH_{2.25}$ hydride is formed at 304 °C on heating. On cooling, the hydride absorbs more hydrogen (especially at around 190 °C) and the final composition at RT becomes $SmH_{2.63}$. In the cases of Sm powder experiments, the hydrogen absorption temperature was found always to be between 300 and 330 °C.

Different hydrogen absorption temperatures were found for the cases where bulk Sm samples were used in the experiments. The ITA isochore traces for the "Sm(bulk) + H_2" system are shown in Fig. 4 for three separate bulk samples weighting 4.65, 2.8 and 2.2 mg,

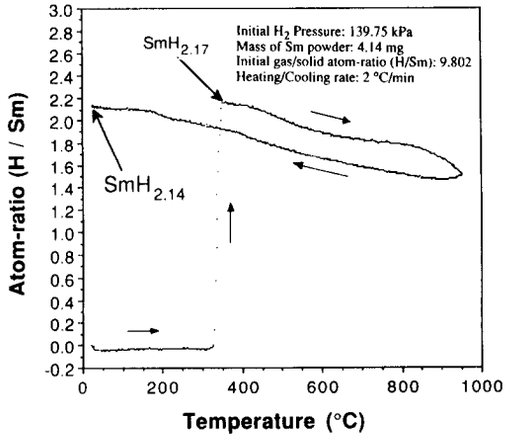

Fig. 2. ITA isochore for the "Sm(powder) + H_2" system; the final RT Sm hydride composition is $SmH_{2.14}$.

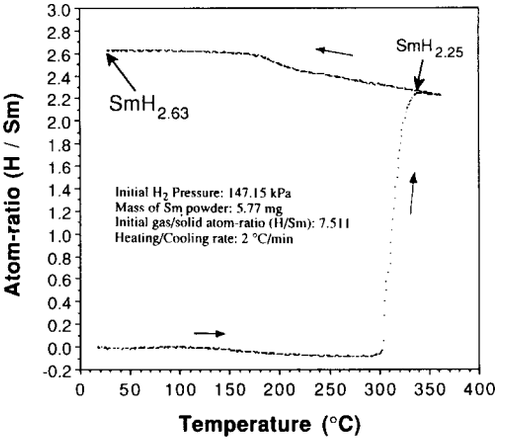

Fig. 3. ITA isochore for the "Sm(powder) + H_2" system by heating up to 360 °C only; the final RT Sm hydride composition is $SmH_{2.63}$.

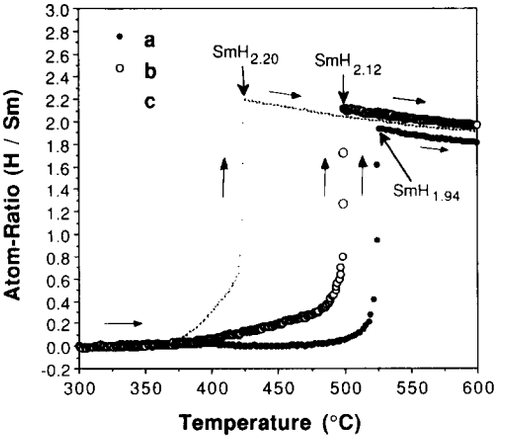

Fig. 4. ITA isochores for the "Sm(bulk, single piece) + H_2" system in the case of three separate samples of different mass: (a) $m = 2.20$ mg, $P_0 = 145.72$ kPa, $(H/Sm)_0 = 18.805$, (b) $m = 2.80$ mg, $P_0 = 142.31$ kPa, $(H/Sm)_0 = 14.311$ and (c) $m = 4.65$ mg, $P_0 = 145.11$ kPa, $(H/Sm)_0 = 8.804$.

respectively. The hydrogen absorption temperatures (steepest rise in hydrogen concentration) were found to be 423, 495 and 524 °C, respectively. In these samples, hydrogenation begins gradually from lower temperatures up to a temperature where it then proceeds rapidly. Also, as the hydrogen absorption temperature increases, the instantly produced Sm hydride contains less hydrogen (see Fig. 4).

The hydrogen absorption temperatures for the Sm powder were found always to be lower than those of the bulk samples. This can be attributed to the fact that the powder samples have much higher surface area available (as compared with bulk samples) for the hydrogen dissociation which occurs before diffusion; the greater degree of surface contamination of the Sm powder may have some effect although it was not confirmed. The large variation (up to 100 °C) in the hydrogen absorption temperatures of the bulk Sm samples, may be due to the different degree of surface structural deformation in each individual sample. Smaller samples (single pieces) exhibit higher hydrogen absorption temperatures possibly due to heavy deformation during the cutting process. The shift in the hydrogen absorption temperature is much less (up to 30 °C) in the case of the powder Sm samples. That is because in general, powder samples do not differ much. The abruptness of the hydrogen absorption may suggest that the reaction of Sm with H_2 is not diffusion controlled; once the "surface resistance" is overcome, absorption occurs quite rapidly. The gradual H_2 absorption observed prior to the abrupt H_2 absorption in the case of the bulk Sm samples is most likely due to the non-uniform surface (local degree of deformation) of these samples. In the case of the powders, the H_2 absorption was observed always to be abrupt since the surface of the particles is uniform with respect to oxygen contamination and degree of structural deformation.

The absorption of hydrogen by samarium involves a change in the crystal structure from rhombohedral (α-Sm) to f.c.c. (Sm hydride). The XRD pattern of the $SmH_{2.63}$ is shown in Fig. 5(a). In addition to the Bragg peaks corresponding to the f.c.c. hydride ($a = 5.366$ Å), there are also Bragg peaks which can be indexed according to the b.c.c. Sm_2O_3 phase ($a = 10.931$ Å). This was an indication that the Sm hydrides are very sensitive to oxygen (atmospheric conditions). In fact, for longer exposure times, the intensity ratio between the Bragg peaks corresponding to Sm_2O_3 and Sm hydride becomes higher (compare Figs. 5(a) and 5(b)). Also the color of the sample turns from black to creamy-yellow. The sensitivity to oxygen is more profound as the value of x (SmH_{2+x}) increases. Sm hydrides which have a composition closer to Sm dihydride showed much less sensitivity to oxidation.

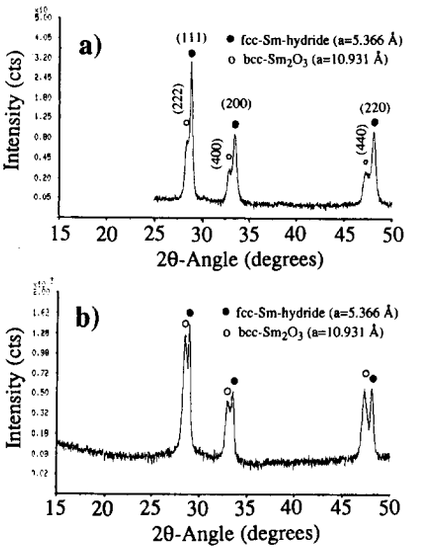

Fig. 5. XRD patterns of the $SmH_{2.63}$ taken (a) immediately after its preparation and (b) after 2 hours' exposure to ambient conditions.

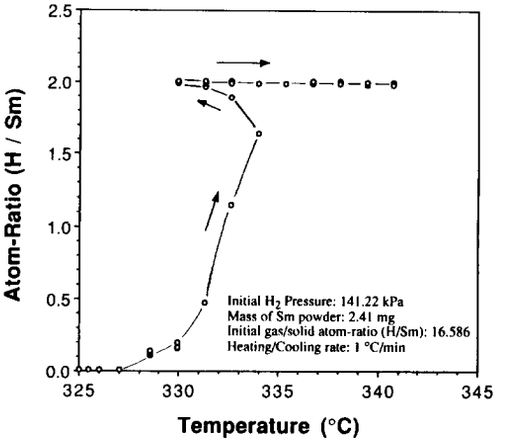

Fig. 6. ITA isochore for the "Sm(powder) + H_2" system demonstrating the exothermic nature of the hydrogen absorption reaction. The time period between data points is 12 seconds.

The hydrogen absorption reaction is very exothermic. This can be detected as an immediate increase followed by a decrease of the temperature, or in general a disturbance of the imposed heating rate during the ITA experiment. This is demonstrated in the ITA isochore trace of the "Sm(powder) + H_2" system shown in Fig. 6, and can be explained as follows. The thermocouple of the temperature controller of the furnace is in contact with the outer surface of the quartz tube in the region where the Sm sample is located. During hydrogen absorption, heat is generated. Subsequently, the temperature of the thermocouple increases faster than the imposed rate of heating (1 °C min^{-1}) and therefore, the temperature controller in response cools down the furnace in order to re-establish the imposed heating rate. This observation is very indicative of the

usefulness of the isochoro-thermal analyzer not only in detecting variations in gas densities but also in detecting heats of reactions (exothermic or endothermic). It is worth noting here that the mass of Sm powder used in this ITA isochore trace (Fig. 6) was only 2.41 mg.

The composition of the SmH_{2+x} obtained by the ITA isochores varies with x taking values of between 0 and 0.63, depending on the hydrogenation conditions (especially temperature). This is in agreement with the results obtained by Daou *et al.* [4] who measured x to be up to 0.6. The XRD patterns always showed the presence of an f.c.c. Sm hydride phase accompanied by a b.c.c. Sm_2O_3 phase. The Sm_2O_3 phase was present even when the original Sm hydride was kept under paraffin oil to prevent oxidation. Contrary to the work done by Greis *et al.* [3] and Pebler and Wallace [2], no body centered tetragonal Sm_3H_7 or hexagonal SmH_3 phases were observed. The possibility exists that these phases were oxidized instantly upon exposure to ambient conditions and therefore were not found in the XRD patterns.

The Sm dihydride possesses the f.c.c. CaF_2-type structure with the hydrogen atoms filling all the tetrahedral interstices. The excess hydrogen atoms (for $0 < x < 0.6$) is known to be distributed randomly in the octahedral interstices [2, 4].

3.2.2. Hydrogen desorption and dissociation of Sm dihydride

The ITA isochores of four separate Sm hydride samples are shown in Fig. 7(a–d), and they were obtained under initial vacuum conditions. Most of the Sm hydrides

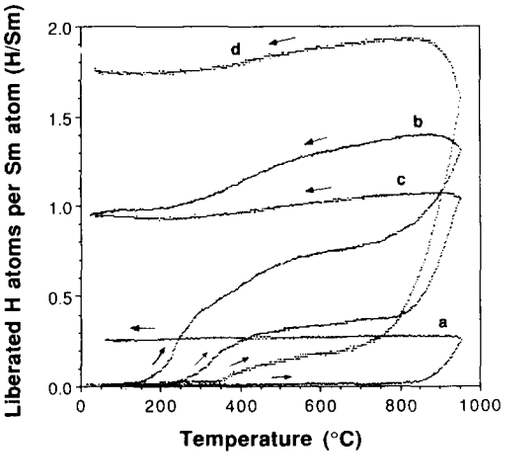

Fig. 7. ITA isochores for the "Sm-hydride + vacuum" system. The compositions of the Sm hydrides were (a) $SmH_{0.82}$ (mixture of 41 mol.% SmH_2 + 59 mol.% Sm), (b) $SmH_{2.63}$, (c) $SmH_{2.14}$ treated under continuous vacuum at 300 °C for 1 hour, and (d) $SmH_{2.6}$ treated under continuous vacuum at 400 °C for 4 hours. The characteristics of each of the samples are listed in Table 1.

(samples (a), (b) and (c)) were prepared inside the ITA apparatus in order to control the final hydrogen composition and more importantly to avoid exposure to oxygen. The Sm hydrides prepared outside of the ITA apparatus (sample (d)) were handled carefully, but a temporary (10 minutes) exposure to ambient conditions was unavoidable. Nevertheless, no visible oxidation was observed for these samples (their color remained black). The process history and other characteristics of each of the Sm hydride samples (a–d) used to obtain the ITA traces (Fig. 7) are listed in Table 1.

Hydrogen atoms located in the octahedral interstices begin to desorb at temperatures as low as 150 °C (Fig. 7(b)). By the time a temperature of 400 °C is reached most of the hydrogen atoms in the octahedral sites were desorbed. This was concluded by comparing the original hydrogen concentration of sample (a) ($SmH_{2.63}$) with that of the hydride at 400 °C (≈ 0.63 H/Sm desorbed) as shown in Fig. 7(b). Meanwhile, hydrogen atoms in the tetrahedral sites begin also to desorb gradually at about 320 °C as shown in Fig. 7(d). Sample (d) is expected to contain only tetrahedrally situated H atoms since the $SmH_{2.6}$ was subjected to vacuum at 400 °C prior to the ITA experiment (Fig. 7(d)). Sample (c) was subjected to vacuum at 300 °C prior to the ITA experiment (Fig. 7(c)) and therefore it still contains some octahedral H atoms. Consequently, desorption of H atoms in sample (c) begins at 220 °C, which is between the desorption temperatures corresponding to samples (b) and (d).

The ITA isochores obtained for samples (a)–(d) suggest that the hydrogen atoms in the tetrahedral sites begin to desorb gradually from 320 up to about 725 °C, where the dissociation of Sm dihydride into $Sm + H_2$ initiates and proceeds rapidly at about 850 °C. The occurrence of the dissociation reaction is clearly shown for sample (a) in Fig. 7(a). The overall composition of sample (a) is $SmH_{0.82}$ (Fig. 8). According to the Sm–H binary phase diagram [1], this composition falls inside the equilibrium phase boundaries of α-Sm and Sm dihydride ($SmH_{\sim 2}$). As a result, sample (a) contains a mixture of Sm dihydride and Sm. Therefore, essentially little or no desorption (retaining the f.c.c. structure) of H atoms occurs in this sample, and the dissociation reaction is selectively isolated and can be seen clearly. The dissociation of Sm dihydride can be seen occurring not only under vacuum but also under the presence of hydrogen gas (*i.e.* Fig. 2). It is worth noticing here that the dissociation of Sm dihydride occurs at about the same temperature as Sm vaporization. ITA isochore traces obtained for pure Sm powder under vacuum showed that the contribution of Sm vaporization to the steep rise in the concentration of the gaseous species in the ITA isochore traces (shown in Fig. 7) is relatively

TABLE 1. Process history of the Sm hydrides (a, b, c and d) prepared for obtaining the ITA isochore traces shown in Fig. 7

ITA isochore trace in Fig. 7 Sample	Preparation of SmH_{2+x} ITA	Heating and cooling rate (°C min^{-1})	Room temperature composition of SmH_{2+x}	Final heat treatment before ITA in vacuum is taken
a	Figure 8 (bulk)	2.5	$x=0.0$ (41 mol.% SmH_2+59 mol% Sm)	none
b	Figure 3 (powder)	2.0	$x=0.63$	none
c	Figure 2 (powder)	2.0	$x=0.14$	300 °C (1 h) under continuous vacuum
d	400 °C (2 h) under H_2 flow (powder)	2.0	Estimated to be $x\approx0.6$	400 °C (4 h) under continuous vacuum

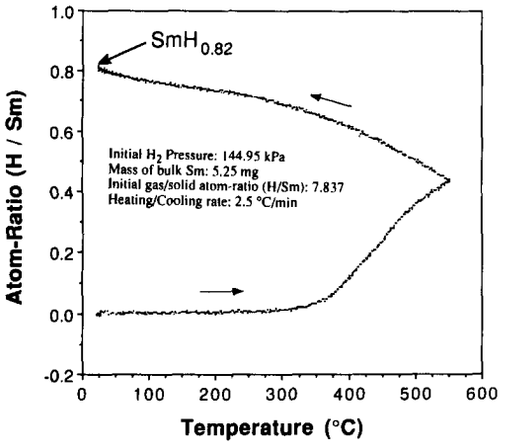

Fig. 8. ITA isochore for the "Sm(bulk)+H_2" system; the final RT composition of the Sm hydride is $SmH_{0.82}$ (mixture of 41 mol.% SmH_2+59 mol.% Sm). This sample was used to obtain the ITA isochore shown in Fig. 7(a).

small. The reason is because the Sm vapors condense almost instantly on the colder part of the quartz tube inside of which the reaction took place.

Information obtained from the study of hydrogen absorption by Sm, hydrogen desorption by Sm hydrides, as well as the dissociation characteristics of Sm dihydride is very important for the hydrogen treatment process (HDDR) used to prepare permanent magnets and more specifically to prepare Sm_2Fe_{17} nitride-based permanent magnets. The present study shows that the recombination process (Sm hydride + α-Fe $\leftrightarrow$ $Sm_2Fe_{17}+H_2$) can be initiated at temperatures close to 725 °C (under vacuum), which is about the temperature where dissociation of the Sm dihydride begins. Under argon gas flow conditions one might expect the recombination temperature to shift higher. In fact, current application of the HDDR process in our laboratory [18], shows that recombination is initiated at 725 °C under vacuum and indeed at higher temperatures ($\approx$800 °C) under argon gas flow conditions.

3.3. Reaction of samarium with nitrogen

3.3.1. Nitrogenation

The ITA isochore trace of the "Sm(powder)+N_2" system is shown in Fig. 9. It suggests that by heating the Sm powder under nitrogen gas at the rate of 5 °C min^{-1} up to 950 °C and cooling to RT, only 51 mol.% of SmN forms. An ITA isochore trace of the "Sm(powder)+N_2" system obtained at a constant temperature of 850 °C for 12 hours (Fig. 10) resulted in 80 mol.% conversion to SmN. Consequently, the reaction rate of Sm with N_2 is very low. In fact, when a bulk piece of Sm metal ($\approx$1 mm^3) was used instead of powder, only 4 mol.% of Sm was converted to SmN at the surface. The reaction of Sm with N_2 involves a change in the crystal structure from rhombohedral (α-Sm) to f.c.c. NaCl-type (SmN). This may require long

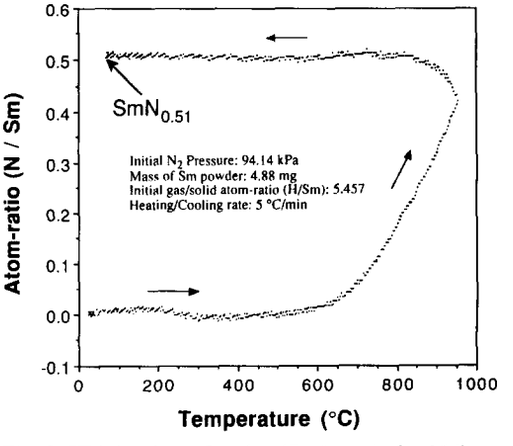

Fig. 9. ITA isochore for the "Sm(powder)+N_2" system; the final composition was 51 mol.% SmN+49 mol.% Sm.

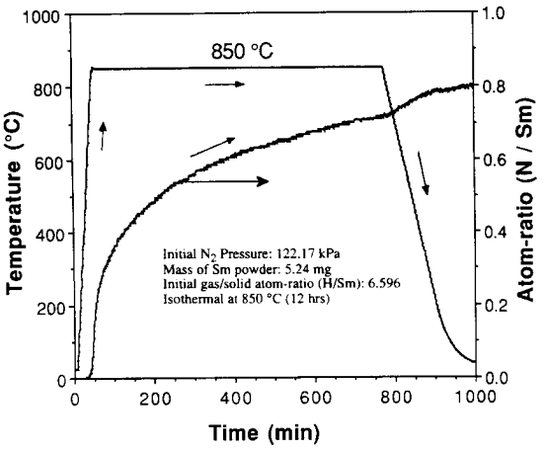

Fig. 10. ITA isochore for the "Sm(powder) + N_2" system obtained isothermally at 850 °C for 12 hours; the final composition was 80 mol.% SmN + 20 mol.% Sm.

distance diffusion of the N atoms in the solid. Apparently, the slow diffusion of the N atoms is the major obstacle to the formation of SmN. Nitrogen diffusion in solids is found to be slow in other cases too where a change of crystal structure does not occur (*i.e.* diffusion of nitrogen into the Sm_2Fe_{17} structure [20, 21]).

Heat treatment experiments of SmN under vacuum showed that SmN is a very stable compound resisting dissociation at temperatures as high as 1000 °C (the highest temperature tried in this study). Eick *et al.* [6] reported that SmN resists dissociation up to 1600 °C.

3.3.2. Decomposition of SmN under ambient conditions

The XRD pattern of a sample prepared by nitrogenation of Sm powder at 850 °C for 12 hours is shown in Fig. 11(a), and it was obtained immediately after its preparation. The sample contains mostly SmN ($a = 5.018$ Å) and unreacted α-Sm together with some b.c.c. Sm_2O_3. The XRD patterns of the same sample exposed to ambient conditions for 30 minutes and for one day are shown in Figs. 11(b) and 11(c), respectively. After 30 minutes exposure to ambient conditions (Fig. 11(b)), the concentration of SmN becomes noticeably less. On the other hand, the b.c.c. Sm_2O_3 concentration increases. Exposure of the sample for one day caused the complete decomposition of SmN into b.c.c. Sm_2O_3 and mostly into hexagonal $Sm(OH)_3$ ($a = 6.36$ Å, $c = 3.66$ Å). During the exposure of SmN in the atmosphere, the smell of ammonia was evident. Therefore, it is concluded that the decomposition of SmN was due to its hydrolyzation in the presence of atmospheric moisture according to the following reactions:

$$2SmN + 3H_2O \longleftrightarrow Sm_2O_3 + 2NH_3 \quad \text{for short times}$$

$$SmN + 3H_2O \longleftrightarrow Sm(OH)_3 + NH_3 \quad \text{for long times}$$

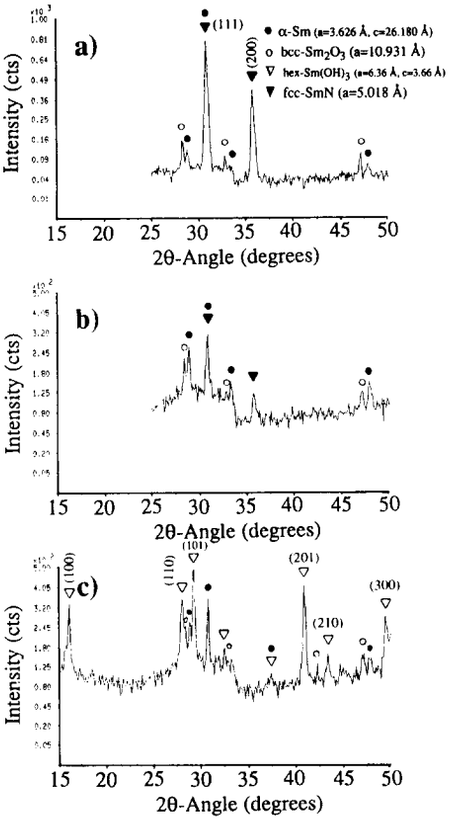

Fig. 11. XRD patterns obtained for the SmN prepared by nitrogenation of Sm powder at 850 °C for 12 hours: (a) immediately after preparation, (b) after 30 minutes exposure to ambient conditions, and (c) after one day exposure to ambient conditions.

The above decomposition scheme was also reported by Eick *et al.* [6], who in addition observed the presence of some SmO(OH) phase in such samples.

The hydrolyzation of SmN may be proven to be very important in future studies on the corrosion resistance of Sm_2Fe_{17} nitride-based permanent magnets, which, depending on the preparation conditions, may contain some SmN as a by-product.

4. Summary

The reaction kinetics between samarium and hydrogen or nitrogen have been studied. Hydrogen absorption is strongly exothermic and occurs rapidly at temperatures between 300 and 525 °C dependent on whether powder or bulk Sm metal is used. The composition of the hydrides was found to vary between 2 and 2.63 H atoms per Sm atom, depending on the hydrogenation conditions. The Sm hydrides exhibit an f.c.c. CaF_2-type of crystal structure with the H atoms occupying all the tetrahedral and a portion of the octahedral interstices. Upon heat treatment under vacuum, the hydrogen atoms in the octahedral sites begin to desorb at about 150

°C with subsequent desorption of the hydrogen atoms in the tetrahedral sites at about 320 °C. The desorption of H atoms continues gradually up to a temperature of 725 °C, where the dissociation of Sm dihydride into elemental Sm and hydrogen gas begins to take place (accelerating at the temperature of about 850 °C). The Sm hydrides decompose partially into b.c.c. Sm_2O_3 under ambient conditions.

The results of hydrogen absorption by Sm, hydrogen desorption from Sm hydrides and dissociation of Sm dihydride provide useful information for the better understanding of the hydrogen treatment process (HDDR) used for the preparation of Sm_2Fe_{17} nitride-based permanent magnets.

The reaction rate between samarium and nitrogen to form SmN was found to be low due to the slow diffusion of N atoms into the solid. Upon exposure of SmN to atmospheric conditions (moisture), it hydrolyzes into b.c.c. Sm_2O_3, hex-$Sm(OH)_3$ and NH_3. This may be proven to be of great importance in the study of corrosion resistance of Sm_2Fe_{17} nitride-based permanent magnets, which may contain some SmN as a by-product, depending on the preparation conditions.

Heat treatment of Sm metal under vacuum or argon flow results in the formation of Sm oxide surface layers. Such oxides were found to be f.c.c. SmO, b.c.c. Sm_2O_3 and monoclinic Sm_2O_3. This indicates the sensitivity of Sm to oxygen and the special conditions that one has to adopt in order to minimize the oxidation of Sm during processes such as MA and HDDR, as applied to the preparation of Sm_2Fe_{17} nitride-based permanent magnets.

References

1 B. J. Beaudry and K. A. Gschneidner, Jr., in G. J. MacCarthy and J. J. Rhyne (eds.), Rare earth in modern science and technology, *Rare Earth Research Conference,* Plenum, New York, 1978, pp. 303–307.
2 A. Pebler and W. E. Wallace, *J. Phys. Chem., 66* (1962) 148.
3 Ortwin Greis, Peter Knappe and Horst Muller, *J. Solid State Chem., 39* (1981) 49.
4 J. N. Daou, P. Vajda and J. P. Burger, *Solid State Commun., 71* (1989) 1145.
5 O. J. Zogal and Ph. I'. Heritier, *J. Alloys Comp., 177* (1991) 83.
6 H. A. Eick, N. C. Baenziger and L. Eyring, *J. Am. Chem. Soc., 78* (1956) 5987.
7 H. A. Eick, N. C. Baenziger and L. Eyring, *J. Am. Chem. Soc., 78* (1956) 5147.
8 B. M. S. Bist, J. Kumar and O. Srivastava, *Phys. Status Solidi A, 14* (1972) 197.
9 PDF No. 15-813, JCPDS-International Centre for Diffraction Data, Park Lane, Swarthmore, PA, 1972, p. 1052.
10 PDF No. 25-749, JCPDS-International Centre for Diffraction Data, Park Lane, Swarthmore, PA, 1984, p. 259.
11 J. M. D. Coey, Hong Sun and Y. Otani, *A New Family of Rare Earth Iron Nitrides,* in S. G. Sankar (ed.), *Proceedings of the Sixth International Symposium on Magnetic Anisotropy and Coercivity in Rare Earth-Transition Metal Alloys, Pittsburgh, PA, October 25, 1990,* p. 36.
12 K. Schnitzke, L. Schultz, J. Wecker and M. Katter, *Appl. Phys. Lett., 57* (1990) 2853.
13 M. Endoh, M. Iwata and M. Tokunaga, *J. Appl. Phys., 70* (1991) 6030.
14 C. N. Christodoulou and T. Takeshita, Rapidly quenched Sm_2Fe_{17}-nitride-based permanent magnets, presented in the meeting of *The Rare Earth Society of Japan,* Tokyo, Japan, July 24, 1991, unpublished results.
15 M. Katter, J. Wecker and L. Schultz, *J. Appl. Phys., 70* (1991) 3188.
16 J. M. D. Coey and H. Sun, *J. Magn. Magn. Mater., 87* (1990) L251.
17 M. Q. Huang, L. Y. Zhang, B. M. Ma, Y. Zheng, J. M. Elbicki, W. E. Wallace and S. G. Sankar, *J. Appl. Phys., 70* (1991) 6027.
18 C. N. Christodoulou and T. Takeshita, *Sm_2Fe_{17}-nitride-based permanent magnets prepared by HDDR,* 1991, unpublished results.
19 H. Nakamura, K. Kurihara, T. Tatsuki, S. Sugimoto, M. Okada and M. Homma, *Variation of Magnetic Properties of $Sm_2Fe_{17}N_x$ Alloys by Hydrogen Treatment, Digests of the 15th Annual Conference on Magnetics in Japan, October 29–November 1, 1991,* Magnetic Society, Ibaraki, Japan, p. 379.
20 J. M. D. Coey, J. F. Lawler, Hong Sun and J. E. M. Allan, *J. Appl. Phys., 69* (1991) 3007.
21 T. Mukai and T. Fujimoto, *J. Magn. Magn. Mater., 103* (1992) 165.
22 M. Q. Huang, B. M. Ma, W. E. Wallace and S. G. Sankar, *Magnetic Properties and Structure of Nitrogenated $R_2(Fe,Co)_{17}$ Intermetallic Compounds,* in S. G. Sankar (ed.), *Proceedings of the Sixth International Symposium on Magnetic Anisotropy and Coercivity in Rare Earth-Transition Metal Alloys, Pittsburg, PA, October 25, 1990,* p. 204.
23 L. Y. Zhang, Y. Zheng and W. E. Wallace, *Magnetization and PCI's of Nitrogenated $R_2(Fe,Co)_{17}$ Systems,* in S. G. Sankar (ed.), *Proceedings of the Sixth International Symposium on Magnetic Anisotropy and Coercivity in Rare Earth-Transition Metal Alloys, Pittsburgh, PA, October 25, 1990,* p. 219.
24 K. H. J. Buschow, R. Coehoorn, D. B. de Mooij, K. de Waard and T. H. Jacobs, *J. Magn. Magn. Mater., 92* (1990) L35.
25 J. M. D. Coey, Hong Sun and D. P. F. Hurley, *J. Magn. Magn. Mater., 101* (1991) 310.
26 M. Q. Huang, Y. Zheng, K. Miller, J. M. Elbicki and S. G. Sankar, *J. Appl. Phys., 70* (1991) 6024.
27 D. P. F. Hurley and J. M. D. Coey, *J. Magn. Magn. Mater., 99* (1991) 229.
28 F. H. Ellinger and W. H. Zachariasen, *J. Am. Chem. Soc., 75* (1953) 5650.